

Determination of stress-coefficient of magnetoelastic anisotropy in flexible amorphous CoFeB film by anisotropic magnetoresistance

Xingcheng Wen,^{1,2,3} Baomin Wang,^{2,3,a)} Ping Sheng,^{2,3,4} Shuai Hu,^{2,3,4} Huali Yang,^{2,3} Ke Pei,^{2,3,5} Qingfeng Zhan,^{2,3} Weixing Xia,^{2,3} Hui Xu,^{1,a)} and Run-Wei Li^{2,3,a)}

¹*Institute of Materials Science, School of Materials Science and Engineering, Shanghai University, Shanghai 200072, People's Republic of China*

²*CAS Key Laboratory of Magnetic Materials and Devices, Ningbo Institute of Materials Technology and Engineering, Chinese Academy of Sciences, Ningbo 315201, People's Republic of China*

³*Zhejiang Province Key Laboratory of Magnetic Materials and Application Technology, Ningbo Institute of Materials Technology and Engineering, Chinese Academy of Sciences, Ningbo 315201, People's Republic of China*

⁴*Nano Science and Technology Institute, University of Science and Technology of China, Suzhou 215123, People's Republic of China*

⁵*Faculty of Materials Science and Chemical Engineering, Ningbo University, Ningbo 315211, People's Republic of China*

(Received 8 August 2017; accepted 23 September 2017; published online 3 October 2017)

Flexible magnetic devices are one of the indispensable flexible devices. However, the deformation of the magnetic devices will change the magnetic anisotropy of magnetic materials due to magnetoelastic anisotropy, which will decrease the performance of the devices. Therefore, it is essential to determine the stress-coefficient of magnetoelastic anisotropy in magnetic materials. Here, the magnetic anisotropy constants of an amorphous CoFeB film on a flexible polyvinylidene fluoride (PVDF) substrate in different stress states were quantitatively investigated by anisotropic magnetoresistance (AMR). The enhanced magnetic anisotropy of the CoFeB film at reduced temperature is due to magnetoelastic anisotropy induced by anisotropic thermal expansion of the PVDF substrate. Through fitting the AMR curves under variant fields in different stress states, the stress-coefficient of magnetoelastic anisotropy in the amorphous CoFeB film is obtained to be $170.7 \times 10^3 \text{ erg cm}^{-3} \text{ GPa}^{-1}$. Published by AIP Publishing. <https://doi.org/10.1063/1.4999493>

Recently, flexible devices on plastic substrates have shown promise in applications including disposable electronics, smart cards, light-emitting diodes, signage, wearable electronics, and sensors.^{1–4} As a necessary part of flexible equipment, flexible magnetic devices have attracted wide attention.⁵ A kind of important magnetic device is based on the giant magnetoresistance (GMR) effect or tunneling magnetoresistance (TMR) effect,^{6,7} which is dependent on the relative magnetization direction between two neighboring ferromagnetic (FM) layers. Co₄₀Fe₄₀B₂₀ (CoFeB) films have been used widely for the FM layers in TMR based magnetic devices because of a higher spin polarization.^{8,9} However, the magnetic anisotropy of CoFeB can be tuned by applied stress due to magnetoelastic anisotropy, which will change the magnetization direction of FM layers.^{10–12} Thus, determination of the stress-coefficient of the magnetoelastic anisotropy constant in magnetic thin films is crucially important not only to the fundamental magnetism but also to designing flexible magnetic devices. Up to date, various methods, such as torque measurement,¹³ ferromagnetic resonance,¹⁴ transverse biased initial inverse susceptibility and torque measurements,¹⁵ rotational magneto-optic Kerr effect,¹⁶ and magnetotransport measurements,^{17,18} have been developed to determine the magnetic anisotropy constant. Among them, anisotropic magnetoresistance (AMR) measurements have been proven to be a simple and effective

probe to determine the anisotropy energies in magnetic films.^{17,19,20}

In this work, we determined the stress-coefficient of magnetoelastic anisotropy in amorphous CoFeB films by AMR. The amorphous CoFeB films were deposited on the flexible polyvinylidene fluoride (PVDF) substrate, which has an anisotropic thermal expansion. The stress on CoFeB films was applied through changing the temperature of the substrates. On the basis of AMR curves, the angle between the magnetization and magnetic field can be obtained, and hence, the normalized magnetic torque can be derived. The magnetic anisotropy constant was precisely obtained by fitting the normalized magnetic torque curves. Then, the stress-coefficient of magnetoelastic anisotropy in the amorphous CoFeB film was obtained by fitting the magnetic anisotropy constants in different stress states.

Ta(2 nm)/CoFeB(40 nm)/Ta(4 nm) were deposited on 50 μm thick PVDF and Si substrates by dc magnetron sputtering at room temperature. Before the deposition, the substrates were cleaned ultrasonically in ethanol and then dried with nitrogen gas. The base pressure of the sputtering chamber was below 5×10^{-8} Torr. During deposition, the Ar flow was kept at 30 sccm and the pressure was set at 3.0×10^{-3} Torr. The deposition power was kept at 100 W. The deposition rate was 3.3 nm/min. Prior to taking out from the chamber, the 2 nm Ta layer was deposited on CoFeB films to prevent oxidation. The angular dependence of hysteresis loops at room temperature was measured using a vibrating sample magnetometer (VSM, Lakeshore 7410). The transmission electron microscope

^{a)}Authors to whom correspondence should be addressed: wangbaomin@nimte.ac.cn; huixu8888@shu.edu.cn; and runweili@nimte.ac.cn

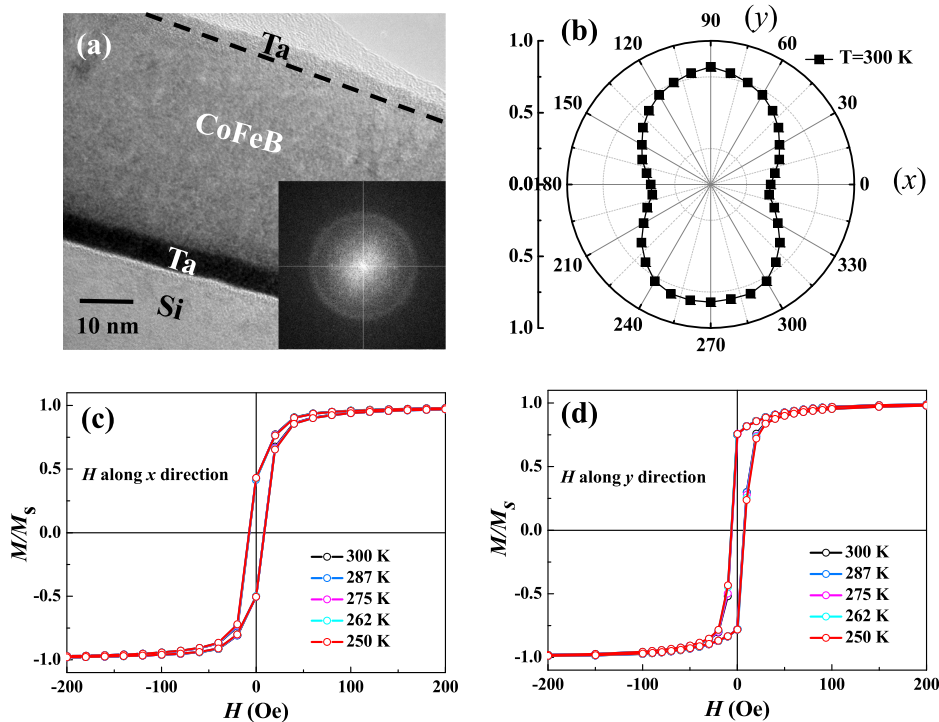


FIG. 1. (a) TEM image of the as-deposited 40 nm CoFeB film on Si. The inset is the FFT image of CoFeB. (b) Angular dependence of normalized M_r/M_s at room temperature; (c) and (d) M - H hysteresis loops at different temperatures along x and y directions, respectively.

(TEM) was used to observe the microstructure of CoFeB films. A quantum design superconducting quantum interference device-vibrating sample magnetometer (SQUID-VSM) was employed to measure the magnetic hysteresis loops for the magnetic film in the temperature range of 250 to 300 K. AMR was carried out using standard four-probe contacts in an Oxford Instruments system equipped with a motorized sample rotator, in which the magnetic field is up to 12 T and the temperature can be changed from 2 to 400 K.

Figure 1(a) shows the cross-sectional TEM image of the as-deposited CoFeB film on Si. CoFeB has an amorphous structure, which can be observed from the corresponding fast Fourier transform (FFT) image [inset of Fig. 1(a)]. In order to check the in-plane anisotropy, the angular dependence of the magnetic hysteresis loops for the CoFeB film on Si was measured at 300 K by VSM. Figure 1(b) shows the angular dependence of normalized remanent magnetization (M_r/M_s), which oscillates with 180° periodicity showing a uniaxial anisotropy with the easy axis along the y direction. The film has a weak uniaxial anisotropy because of the stray field in the process of film growth. In order to study the temperature dependence of magnetic anisotropy in the amorphous CoFeB film on Si, we measured the magnetic hysteresis loops along the hard (x direction) and easy axes (y direction) at different temperatures [Figs. 1(c) and 1(d)]. There is no obvious change of hysteresis loops from 300 to 250 K, indicating that the magnetic anisotropy of the amorphous CoFeB thin film gives a negligible change during this temperature range.

In order to induce magnetoelastic anisotropy in the amorphous CoFeB film, we deposit the film on the PVDF substrate, which has an anisotropic thermal expansion coefficient, $\alpha_{31} = -13$ ppm/K, and $\alpha_{32} = -145$ ppm/K.^{21,22} The uniaxial stress will be applied on CoFeB films by changing the temperature of the PVDF substrate [Fig. 2(a)]. We define x and y directions along the edge of the substrate with thermal expansion coefficients of α_{31} and α_{32} , respectively. Figure 2(b)

shows the angular dependence of normalized remanent magnetization (M_r/M_s), which oscillates with 180° periodicity showing a uniaxial anisotropy with the easy axis along the y direction. Figure 2(c) shows the in plane magnetic hysteresis loops measured with H along the x direction. The magnetic hysteresis loop becomes slanted as the temperature is decreased. On the other hand, the easy axis magnetic hysteresis loop along the y direction becomes squarer [Fig. 2(d)]. These results are different from that observed in amorphous CoFeB on the Si substrate [Figs. 1(c) and 1(d)], indicating that enhanced magnetic anisotropy is due to magnetoelastic anisotropy induced by anisotropic thermal expansion of the PVDF substrate.

To obtain the magnetic anisotropy constant of the amorphous CoFeB film, we carried out AMR measurements. The AMR can be expressed as^{17,18,23,24}

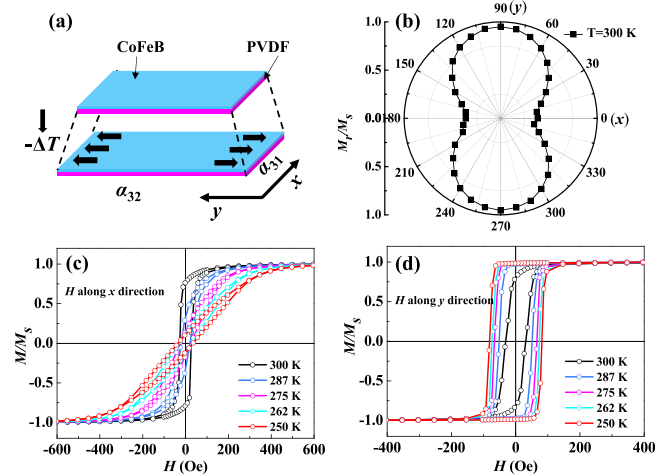


FIG. 2. (a) Schematic view of the stress applied on the amorphous CoFeB film through the anisotropic thermal expansion of the PVDF substrate. (b) Angular dependence of normalized M_r/M_s at room temperature. (c) and (d) M - H hysteresis loops at different temperatures for H along x and y directions, respectively.

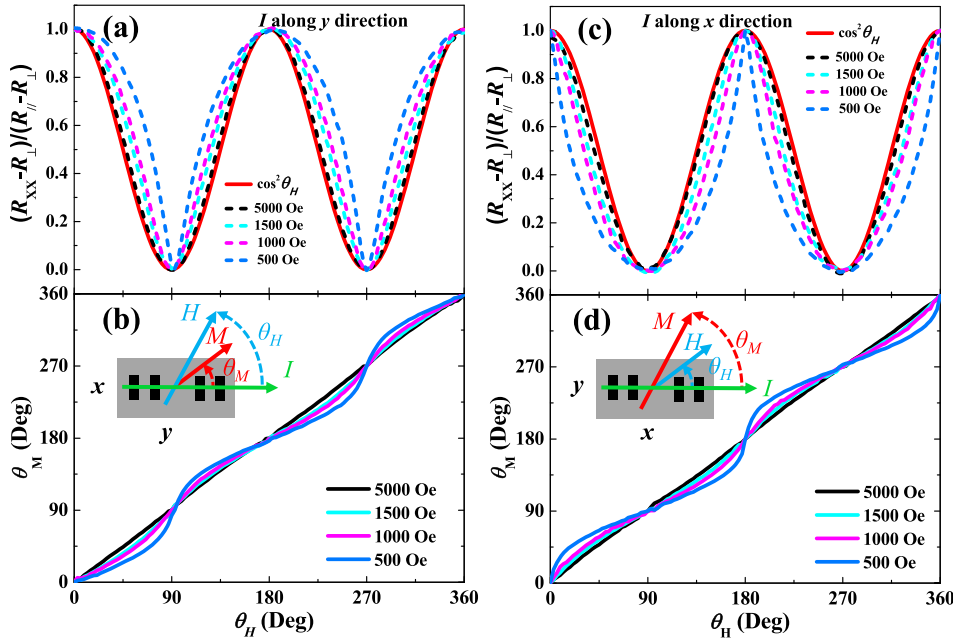


FIG. 3. (a) and (b) AMR curves and angular dependence of the correlations between θ_H and θ_M at 250 K for I along the y direction. (c) and (d) AMR curves and angular dependence of the correlations between θ_H and θ_M at 250 K for I along the x direction.

$$R_{xx} = R_{\perp} + (R_{\parallel} - R_{\perp}) \cos^2 \theta_M, \quad (1)$$

where θ_M is the angle between the magnetization (M) and the current (I), and R_{\parallel} and R_{\perp} are the resistances at $\theta_M = 0^\circ$ and $\theta_M = 90^\circ$, respectively. Figure 3(a) shows in-plane AMR with different applied fields at 250 K with I along the y direction. The AMR curves show an oscillated behavior between the maximum value R_{\parallel} and minimum value R_{\perp} . However, owing to the magnetic anisotropy, M is no longer kept along with the H during rotation, i.e., $\theta_M \neq \theta_H$, θ_H is the angle between the direction of magnetic field H and the direction along the y axis [inset of Figs. 3(b) and 3(d)]. As a result, the AMR curves do not follow the $\cos^2(\theta_H)$ relationship. Obviously, it can be expressed as

$$\theta_M = \arccos \left(\sqrt{\frac{R_{xx} - R_{\perp}}{R_{\parallel} - R_{\perp}}} \right). \quad (2)$$

Figure 3(b) shows the correlation between θ_M and θ_H , which is calculated using Eq. (2). Figures 3(c) and 3(d) show the AMR curves and the correlation between θ_M and θ_H with I along the x direction, respectively. The θ_M versus θ_H curves have 90° phase difference between I along x and y directions. At 250 K, the easy axis of magnetic anisotropy in the CoFeB film is along the y direction due to a tensile stress applied

along this direction [Fig. 2(a)]. The magnetic moments tend to distribute along the direction of the easy axis, resulting in that the θ_M falls behind (pulls ahead) θ_H for I along the y (x) direction at θ_H from 0° to 90° .

On the basis of the angle difference between θ_M and θ_H , we can further calculate the magnetic torque

$$L(\theta_M) = \mu_0 M_s H \sin(\theta_H - \theta_M), \quad (3)$$

where μ_0 is the magnetic permeability and M_s is the saturation magnetization. In order to compare magnetic torques at different fields, the normalized magnetic torque

$$l(\theta_M) = L(\theta_M) / \mu_0 M_s H = \sin(\theta_H - \theta_M). \quad (4)$$

Figures 4(a) and 4(b) show the normalized magnetic torque curves at different external fields for I along y and x directions, respectively. The normalized magnetic torque increases when the applied magnetic field decreases. The torque curves at high magnetic field of 5000 Oe show a smooth behavior, implying that hysteresis is smaller than that obtained at the low field.

For a uniaxial in-plane anisotropy of the CoFeB/PVDF system, the energy per unit area can be expressed as

$$E = K_U \sin^2 \theta_M - \mu_0 M_s H \cos(\theta_H - \theta_M), \quad (5)$$

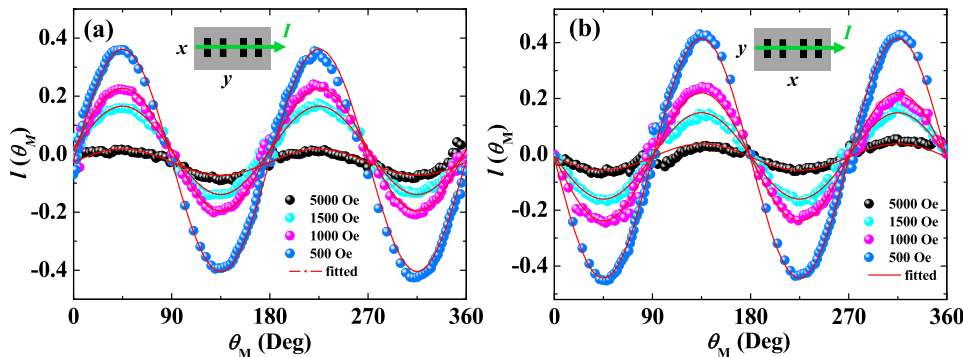


FIG. 4. (a) and (b) Normalized magnetic torque curves at 250 K under different magnetic fields for I along the y and x directions, respectively. The solid lines denote fitting curves using Eq. (6).

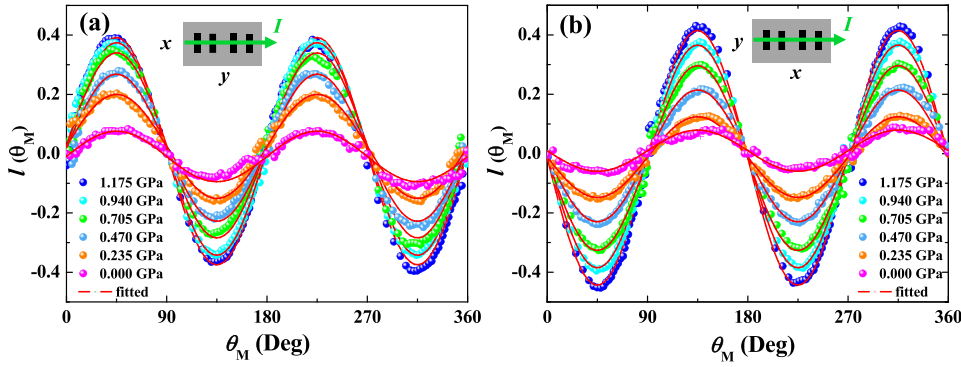


FIG. 5. (a) and (b) Normalized magnetic torque curves in different stress states under $H = 500$ Oe for I along the y and x directions, respectively. The solid lines denote fitting curves using Eq. (6).

where K_u is the magnetic anisotropy constant. In the equilibrium state, the torque acting on M due to H is equal in magnitude to the torque due to the magnetic anisotropies of the sample. According to Eq. (5), the normalized magnetic torque can be written as

$$I(\theta_M) = \sin(\theta_H - \theta_M) = [K_U/(\mu_0MH)]\sin(2\theta_M). \quad (6)$$

By fitting the magnetic torque curve by Eq. (6), we obtain the K_u of the CoFeB film on PVDF at 250 K to be $(2.25 \pm 0.06) \times 10^2$ erg/cm³ and $(2.22 \pm 0.06) \times 10^2$ erg/cm³ for I along y and x directions, respectively.

In order to obtain the stress-coefficient of magnetoelastic anisotropy in the CoFeB film, we measured the AMR curves and calculate the K_u of CoFeB in different stress states. The stress is applied on the film through an anisotropic thermal expansion of the PVDF substrate. The induced stress (σ) can be written as

$$\sigma = \varepsilon E_f / (1 - \nu^2), \quad (7)$$

where E_f is the Young's modulus of the CoFeB film (~ 162 GPa),²⁵ ν is the Poisson ratio of the CoFeB film (~ 0.3),²⁶ ε is the strain, and $\varepsilon = \Delta T(\alpha_{32} - \alpha_{31})$. Figures 5(a) and 5(b) show the typical normalized magnetic torque curves $I(\theta_M)$ with 500 Oe in different stress states for I along y and x directions, respectively. The torque curves clearly show that the anisotropies are uniaxial anisotropy in different stress states. The normalized magnetic torque increases with the increase of applied stress. Figure 6 shows the magnetic

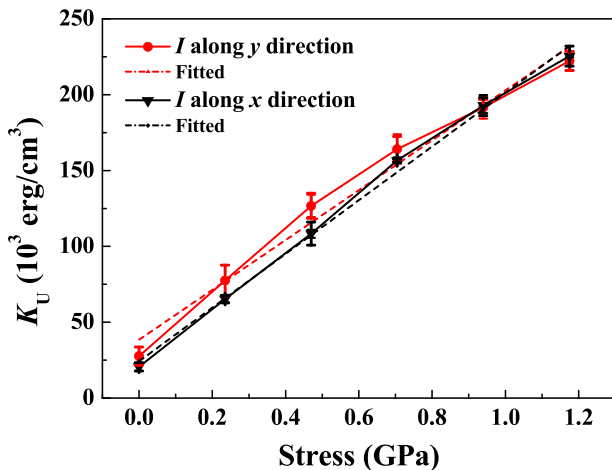


FIG. 6. The magnetic anisotropy constant K_U as a function of the applied stress for I along the y and x directions, respectively. The dotted lines denote the linear fitting curves.

anisotropy constants in various stress states obtained by AMR measurements with I along y and x directions, respectively. The stress dependence of magnetic anisotropy constant has the same tendency for two directions and a variation of stress has a significant effect on the values of K_u . The magnetic anisotropy constant is only about 27.7 ± 5.8 erg/cm³ in the initial state, while it gradually increases with the increasing stress and eventually reaches $(2.22 \pm 0.06) \times 10^2$ erg/cm³ at 1.175 GPa for I along the y direction. The same is for I along the x direction, where the magnetic anisotropy constant increases from initial 20.6 ± 2.5 erg/cm³ to $(2.25 \pm 0.06) \times 10^2$ erg/cm³ at 1.175 GPa. Since the magnetic anisotropy of the amorphous CoFeB thin film on Si shows a negligible change with temperature [Figs. 1(c) and 1(d)], the change of magnetic anisotropy (ΔK_u) of the CoFeB thin film on PVDF comes from the change of magnetoelastic anisotropy (ΔK_σ). The stress-coefficient of magnetoelastic anisotropy ($\Delta K_\sigma / \Delta \sigma$) is deduced to be 164.4×10^3 erg cm⁻³ GPa⁻¹ and 176.9×10^3 erg cm⁻³ GPa⁻¹ for I along y and x directions, respectively [Fig. 6]. Thus, the stress-coefficient of magnetoelastic anisotropy in the amorphous CoFeB film is approximately 170.7×10^3 erg cm⁻³ GPa⁻¹ from averaging the similar value obtained from two direction measurements.

In summary, we fabricated amorphous CoFeB films on the flexible PVDF substrate by dc-sputtering. The magnetoelastic anisotropy in the CoFeB film can be induced by changing the temperature of the PVDF substrate. The magnetic anisotropy constants in different stress states were determined by AMR. The stress-coefficient of magnetoelastic anisotropy in the CoFeB amorphous film is deduced to be 170.7×10^3 erg cm⁻³ GPa⁻¹. This result is useful for evaluating the performance of magnetic devices under flexible conditions and designing the flexible magnetic devices with enhanced performance.

This work was supported by National Key R&D Program of China (2016YFA0201102), the National Natural Science Foundation of China (51571208, 51525103, 11474295, 51471101, and 51401230), the Youth Innovation Promotion Association of the Chinese Academy of Sciences (2016270), the Key Research Program of the Chinese Academy of Sciences (KJZD-EW-M05), MOST 973 of China (2015CB856800), Ningbo Major Project for Science and Technology (2014B11011), Ningbo Science and Technology Innovation Team (2015B11001), and Ningbo Natural Science Foundation (2015A610110).

- ¹H. T. Yi, M. M. Payne, J. E. Anthony, and V. Podzorov, *Nat. Commun.* **3**, 1259 (2012).
- ²X. Wang, Y. Gu, Z. Xiong, Z. Cui, and T. Zhang, *Adv. Mater.* **26**, 1336–1342 (2014).
- ³M. L. Hammock, A. Chortos, B. C. Tee, J. B. Tok, and Z. Bao, *Adv. Mater.* **25**, 5997–6038 (2013).
- ⁴S. R. Forrest, *Nature* **428**, 911–918 (2004).
- ⁵D. Makarov, M. Melzer, D. Karnaushenko, and O. G. Schmidt, *Appl. Phys. Rev.* **3**, 011101 (2016).
- ⁶M. N. Baibich, J. M. Broto, A. Fert, F. N. Van Dau, F. Petroff, P. Etienne, G. Creuzet, A. Friederich, and J. Chazelas, *Phys. Rev. Lett.* **61**, 2472–2475 (1988).
- ⁷G. Binasch, P. Grünberg, F. Saurenbach, and W. Zinn, *Phys. Rev. B* **39**, 4828–4830 (1989).
- ⁸S. S. Parkin, C. Kaiser, A. Panchula, P. M. Rice, B. Hughes, M. Samant, and S. H. Yang, *Nat. Mater.* **3**, 862–867 (2004).
- ⁹S. Ikeda, K. Miura, H. Yamamoto, K. Mizunuma, H. D. Gan, M. Endo, S. Kanai, J. Hayakawa, F. Matsukura, and H. Ohno, *Nat. Mater.* **9**, 721–724 (2010).
- ¹⁰Z. Tang, B. Wang, H. Yang, X. Xu, Y. Liu, D. Sun, L. Xia, Q. Zhan, B. Chen, M. Tang, Y. Zhou, J. Wang, and R. W. Li, *Appl. Phys. Lett.* **105**, 103504 (2014).
- ¹¹Y. Liu, B. Wang, Q. Zhan, Z. Tang, H. Yang, G. Liu, Z. Zuo, X. Zhang, Y. Xie, X. Zhu, B. Chen, J. Wang, and R. W. Li, *Sci. Rep.* **4**, 6615 (2014).
- ¹²G. Yu, Z. Wang, M. Abolfath-Beygi, C. He, X. Li, K. L. Wong, P. Nordeen, H. Wu, P. V. Ong, N. Kioussis, G. P. Carman, X. Han, I. A. Alhomoudi, P. Khalili Amiri, and K. L. Wang, *Appl. Phys. Lett.* **106**, 072402 (2015).
- ¹³S. Yaegashi, T. Kurihara, and K. Satoh, *J. Appl. Phys.* **81**, 6303–6309 (1997).
- ¹⁴S. M. Rezende, J. A. S. Moura, F. M. de Aguiar, and W. H. Schreiner, *Phys. Rev. B* **49**, 15105–15109 (1994).
- ¹⁵G. Garreau, S. Hajjar, J. L. Bubendorff, C. Pirri, D. Berling, A. Mehdaoui, R. Stephan, P. Wetzel, S. Zabrocki, G. Gewinner, S. Boukari, and E. Beaurepaire, *Phys. Rev. B* **71**, 094430 (2005).
- ¹⁶R. Mattheis and G. Quednau, *J. Magn. Magn. Mater.* **205**, 143–150 (1999).
- ¹⁷M. Gruyters, *Phys. Rev. B* **73**, 014404 (2006).
- ¹⁸W. N. Cao, J. Li, G. Chen, J. Zhu, C. R. Hu, and Y. Z. Wu, *Appl. Phys. Lett.* **98**, 262506 (2011).
- ¹⁹E. D. Dahlberg, K. Riggs, and G. A. Prinz, *J. Appl. Phys.* **63**, 4270–4275 (1988).
- ²⁰B. H. Miller and E. D. Dahlberg, *Appl. Phys. Lett.* **69**, 3932–3934 (1996).
- ²¹K. Mori and M. Wuttig, *Appl. Phys. Lett.* **81**, 100–101 (2002).
- ²²Y. Lin, N. Cai, J. Zhai, G. Liu, and C.-W. Nan, *Phys. Rev. B* **72**, 012405 (2005).
- ²³I. N. Krivorotov, C. Leighton, J. Nogués, I. K. Schuller, and E. D. Dahlberg, *Phys. Rev. B* **65**, 100402 (2002).
- ²⁴J. Ye, W. He, Q. Wu, H. L. Liu, X. Q. Zhang, Z. Y. Chen, and Z. H. Cheng, *Sci. Rep.* **3**, 2148 (2013).
- ²⁵A. T. Hindmarch, A. W. Rushforth, R. P. Campion, C. H. Marrows, and B. L. Gallagher, *Phys. Rev. B* **83**, 212404 (2011).
- ²⁶N. Lei, S. Park, P. Lecoeur, D. Ravelosona, C. Chappert, O. Stelmakhovych, and V. Holy, *Phys. Rev. B* **84**, 012404 (2011).